

Catalytic synthesis of nitrogen-doped multi-walled carbon nanotubes using layered double hydroxides as catalyst precursors

YONG CAO, YUN ZHAO, QINGXIA LI and QINGZE JIAO*

School of Chemical Engineering and the Environment, Beijing Institute of Technology,
Beijing 100081, PR China
e-mail: jiaoqz@bit.edu.cn

MS received 22 January 2008; revised 15 November 2008

Abstract. The nitrogen (N)-doped carbon (CN_x) nanotubes were synthesized by pyrolysis of ethylenediamine with Ni_{1.07}Mg_{1.01}AlO_{3.58}, Ni_{1.99}Mg_{0.29}AlO_{3.78}, and Ni_{2.31}Mg_{0.08}AlO_{3.89} mixed oxides as catalysts at 650°C. Those mixed oxides were obtained by calcination of corresponding layered double hydroxide precursors (LDHs). Structure and composition of LDHs and mixed oxides were characterized by X-ray diffraction (XRD) and Inductively coupled plasma spectrum. X-ray photoelectron spectroscopy and transmission electron microscope were used to characterize the N content, proportion of pyridine-like N structure and morphology of CN_x nanotubes. The results showed that the tubes grown with Ni_{2.31}Mg_{0.08}AlO_{3.89} as catalysts had more obvious bamboo-like structure, larger diameter than those grown with Ni_{1.07}Mg_{1.01}AlO_{3.58} and Ni_{1.99}Mg_{0.29}AlO_{3.78}. The N content and proportion of graphitic-like N structures increased with the content of Ni²⁺ increasing in LDH precursors. The morphology, N content and pyridine-like N structures for CN_x nanotubes can be controlled to a certain extent by varying the content of Ni²⁺ in LDH precursors.

Keywords. Layered double hydroxides; N-doped carbon nanotube; pyrolysis; catalyst.

1. Introduction

Layered double hydroxides (LDHs) are composed of charged brucite-like layers of divalent and trivalent metal hydroxides, whose excess positive charge due to the incorporated trivalent metal cation is balanced by anions in the interlayer. LDHs themselves have attracted a great deal of interest as anion exchangers, adsorbents, ionic conductors and antacids¹. Furthermore, the mixed oxides obtained by calcination of LDHs at intermediate temperatures (450–600°C) are of considerable interest in their own right as catalysts and catalyst supports¹. Various transition metal cations introduced into the brucite-like layers of LDHs can be precursors of redox-type centers, showing attractive catalytic activity due to the novel properties of the final catalysts, such as high metal dispersion. Yun Zhao has synthesized the carbon nanosturctures (nanofibres, single-walled and multi-walled carbon nanotubes) using the mixed oxides of Fe_{0.1}Mg₂Al_{0.9}O_{3.45}, Fe_{0.1}Zn₂Al_{0.9}O_{3.45} and Fe_{0.1}Cu₂Al_{0.9}O_{3.45} by calcination of their corresponding LDH precursors as catalysts at 910°C.²

Carbon nanotubes (CNTs) are currently attractive materials for a diverse range of applications because of their extraordinary mechanical and electrical properties.³ The important potential applications include field emission displays⁴ and nanoscale electronic devices.^{5,6} Many of these applications are based on the electrical properties of CNTs, which strongly depend on their helicity and diameter.⁷ Therefore, the control of electrical properties is very important in many applications of CNTs.

Synthesis of N-doped carbon (CN_x) nanotubes has recently been considered as a possible method to control the electrical properties of CNTs in a well-defined way. An enhancement of conductivity is expected, because the additional electrons contributed by the N atom provide electron carriers for the conduction band.⁸ The advantage of such nanotubes is that their conductive properties are primarily determined by the composition and are thus relatively easy to control. CN_x nanotubes are mainly prepared by chemical vapour deposition (CVD), arc discharge, and magnetron sputtering. CVD is considered as the best method for a large-scale production of CNTs. Many research groups have produced CN_x nanotubes

*For correspondence

by CVD using C/N sources.^{9–13} However, almost all the catalysts used to grow CN_x nanotubes are focused on iron, such as ferrocene,⁹ iron phthalocyanine,¹⁰ iron oxide film,¹¹ and iron film.¹² Nickel catalysts are rarely investigated excepting for Ni phthalocyanine (NiC₃₂N₈H₁₆).

CN_x nanotubes synthesized by pyrolyzing NiC₃₂N₈H₁₆ as a starting material has been reported.^{14,15} However, it always requires high purity NiC₃₂N₈H₁₆ and a dual furnace fitted with independent temperature controllers. One heating stage is used to evaporate NiC₃₂N₈H₁₆ and the other stage is used to pyrolyze NiC₃₂N₈H₁₆ to generate the Ni atoms or clusters deposited on the substrate to grow tubes. Another disadvantage is that the growth temperature is required above 800°C. Previous report¹⁴ showed that CNTs could not be synthesized using NiC₃₂N₈H₁₆ at the temperatures below 800°C.

In this paper, we synthesized the CN_x nanotubes by a simple CVD using the mixed oxides containing Ni as catalysts only at 650°C. The lower growth temperature facilitates to form the pyridine-like N structures, which are responsible for the metallic properties of the CN_x nanotubes.⁸ The influence of the content of Ni²⁺ in LDHs on the doped N content and morphology of CN_x nanotubes were investigated.

2. Experimental

2.1 Preparation and calcination of LDHs

LDHs with various Ni content were prepared using a coprecipitation reaction. A 100 mL solution containing Ni(NO₃)₂·6H₂O, Mg(NO₃)₂·6H₂O, and Al(NO₃)₃·9H₂O ([Ni + Mg]/Al = 2.5/1 (molar ratio)) was added, slowly and with vigorous stirring, to another 100 mL solution with NaOH and Na₂CO₃. The resulting slurry was aged at 90°C. The final precipitate was filtered, washed thoroughly with water and dried. Varying the Ni(NO₃)₂·6H₂O and Mg(NO₃)₂·6H₂O content in the solution of nitrates, LDHs with various Ni content were obtained. The mixed oxides were obtained by calcination of LDH precursors at 600°C in air.

2.2 Synthesis of CN_x nanotubes

Synthesis of CN_x nanotubes was carried out in a horizontal furnace. The mixed oxide catalyst (0.50 g) was transferred to a quartz boat and placed in the middle of furnace, which was heated under a flowing Ar (200 mL/min) at a rate of 5 K/min. On reach-

ing 400°C, Ar was switched to H₂ (120 sccm) to reduce the mixed metal oxide. On reaching 650°C, ethylenediamine was pumped into the furnace at a rate of 0.3 mL/min. The reaction was maintained for 40 min, after which the furnace was allowed to cool to room temperature under Ar. CN_x nanotubes were purified by immersing the as-prepared products in a nitric acid solution for 24 h.

2.3 Characterization techniques

The catalysts were characterized by X-ray diffraction (XRD) and inductively coupled plasma spectrum (ICP). The XRD patterns were determined using a X'PERT PRO MPD X-ray diffractometer, using CuKα1 radiation. The generator tension was 40 kV and the generator current was 40 mA. ICP was recorded on a ULTIMA instrument. The samples were dissolved by nitric acid.

Transmission electron microscope (TEM), X-ray photoelectron spectroscopy (XPS), and Raman spectroscopy were used to characterize the purified tubes. The morphology of CN_x nanotubes was examined by TEM using a JEM-1200EX electron microscope. Purified CN_x nanotubes were suspended in ethanol and a drop of the suspension was deposited on a copper grid and the solvent was evaporated. Micrographs were taken at 100 kV. The content and the structure of N in CN_x nanotubes was determined by XPS (Physical electronics PHI 5300) using a vacuum generators XPS system operating with Mg (Kα) radiation. The raw data were correcting for charging using the binding energy of graphite at 284.6 eV. Peak areas were determined after background subtraction using Shirley's method and fitting the spectra with Gaussian curves. The content of N incorporated was calculated from the peak areas of the C1s and N1s peaks after correcting for differences in sensitivity using sensitivity factors of 0.25 and 0.42 for C and N, respectively. Raman spectroscopy was carried out on Renishaw inVia-Reflex instrument using the excitation wavelength of 532 nm.

3. Results and discussion

3.1 ICP and XRD characterization of the catalysts

ICP was employed to measure the metal composition of the prepared LDHs. The results are Ni_{1.07}Mg_{1.01}Al-LDH, Ni_{1.99}Mg_{0.29}Al-LDH, and Ni_{2.31}Mg_{0.08}Al-LDH, respectively. Powder XRD patterns for as-prepared Ni_{1.07}Mg_{1.01}Al-LDH, Ni_{1.99}Mg_{0.29}Al-LDH,

and $\text{Ni}_{2.31}\text{Mg}_{0.08}\text{Al-LDH}$ are shown in figure 1. In each case, the XRD pattern exhibits the characteristic reflections of an LDH material, which shows that it contains hydrotalcite as the main component, exhibiting sharp and symmetric reflections for the basal (003), (006), and (009). The basal spacing obtained from the d_{003} is 0.758, 0.778, and 0.789 nm for as-prepared $\text{Ni}_{1.07}\text{Mg}_{1.01}\text{Al-LDH}$, $\text{Ni}_{1.99}\text{Mg}_{0.29}\text{Al-LDH}$, and $\text{Ni}_{2.31}\text{Mg}_{0.08}\text{Al-LDH}$.

The above LDH samples were calcined at 600°C for 4 h to obtain catalysts used to grow CN_x nanotubes. The powder XRD patterns for the calcined

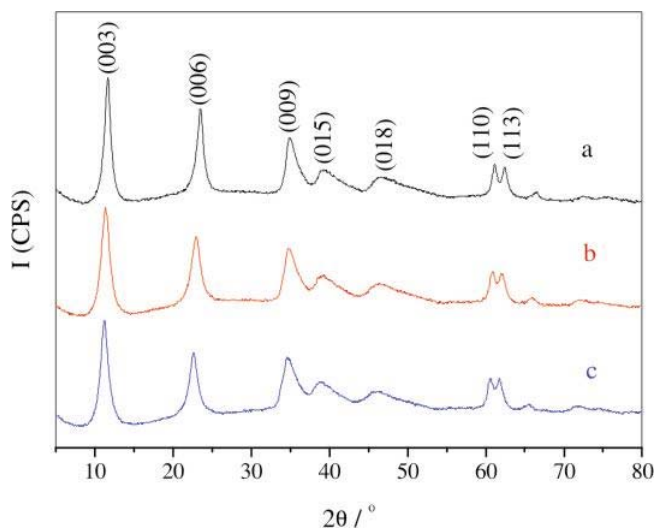


Figure 1. XRD patterns for LDHs with different components: (a) $\text{Ni}_{1.07}\text{Mg}_{1.01}\text{Al-LDH}$, (b) $\text{Ni}_{1.99}\text{Mg}_{0.29}\text{Al-LDH}$ and (c) $\text{Ni}_{2.31}\text{Mg}_{0.08}\text{Al-LDH}$.

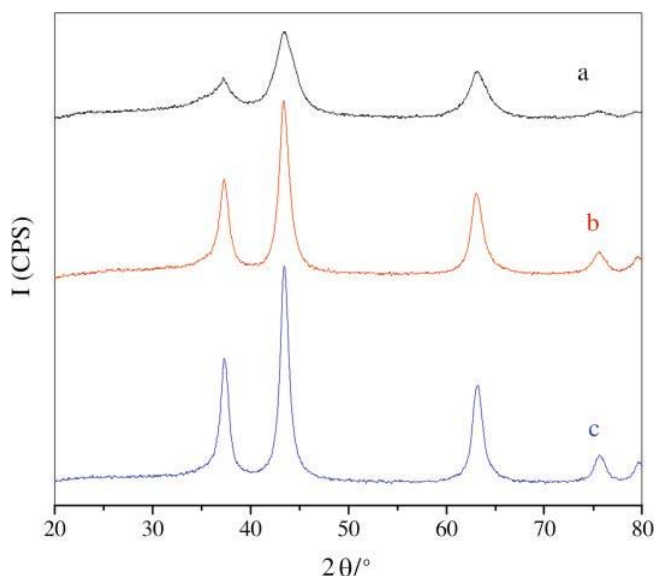


Figure 2. XRD patterns for mixed oxides obtained by calcination of different LDH precursors: (a) $\text{Ni}_{1.07}\text{Mg}_{1.01}\text{AlO}_{3.58}$, (b) $\text{Ni}_{1.99}\text{Mg}_{0.29}\text{AlO}_{3.78}$ (c) $\text{Ni}_{2.31}\text{Mg}_{0.08}\text{AlO}_{3.89}$.

products from the LDH precursors are shown in figure 2. For $\text{Ni}_{1.07}\text{Mg}_{1.01}\text{AlO}_{3.58}$, $\text{Ni}_{1.99}\text{Mg}_{0.29}\text{AlO}_{3.78}$ and $\text{Ni}_{2.31}\text{Mg}_{0.08}\text{AlO}_{3.89}$ samples, XRD patterns show the diffraction peaks of MgO (JCPDS 4520946) and NiO (JCPDS 4721049), which overlap each other. The peaks are broad because of the low crystallinity. This indicates that the calcined products of LDHs are mixed oxides with an MgO-like structure (for $\text{Ni}_{1.07}\text{Mg}_{1.01}\text{AlO}_{3.58}$) or a NiO-like (for $\text{Ni}_{1.99}\text{Mg}_{0.29}\text{AlO}_{3.78}$ and $\text{Ni}_{2.31}\text{Mg}_{0.08}\text{AlO}_{3.89}$) structure as reported by Yun Zhao *et al.*¹⁶

3.2 TEM, XPS, and Raman characterization of CN_x nanotubes

TEM images of CN_x nanotubes prepared with various catalysts are shown in figure 3. The diameter of the tubes grown with $\text{Ni}_{1.07}\text{Mg}_{1.01}\text{AlO}_{3.58}$ and $\text{Ni}_{1.99}\text{Mg}_{0.29}\text{AlO}_{3.78}$ are about 15–50 nm, while the other grown with $\text{Ni}_{2.31}\text{Mg}_{0.08}\text{AlO}_{3.89}$ are about 15–80 nm. Almost all the tubes grown with $\text{Ni}_{2.31}\text{Mg}_{0.08}\text{AlO}_{3.89}$ have an obvious bamboo-like morphology with transverse carbon bridges forming compartments, similar to other reported structures of CN_x nanotubes.^{9–13} But for the tubes grown with $\text{Ni}_{1.07}\text{Mg}_{1.01}\text{AlO}_{3.58}$ and $\text{Ni}_{1.99}\text{Mg}_{0.29}\text{AlO}_{3.78}$, the bamboo-like morphology is unobvious. In addition, the compartment layers of the tubes grown with $\text{Ni}_{2.31}\text{Mg}_{0.08}\text{AlO}_{3.89}$ are thicker and the distance between two adjacent layers becomes longer than those grown with $\text{Ni}_{1.07}\text{Mg}_{1.01}\text{AlO}_{3.58}$ and $\text{Ni}_{1.99}\text{Mg}_{0.29}\text{AlO}_{3.78}$.

XPS analysis was carried out on the CN_x nanotubes grown with various catalysts to look for the content and the structure of N in each product. The C1s and N1s XPS spectra of CN_x nanotubes are shown in figure 4(A) and (B), respectively. All XPS spectra show that the tubes consist of carbon accompanied by traces of N. The N content, which is defined as the $N/(N+C)$ atomic ratio%, was estimated by the area ratio of the C1s and N1s peaks, taking into consideration of their relative sensitivities.

For all XPS spectra, the asymmetric C1s band and N1s band can be observed centered at 284.6 eV and 400.5 eV respectively. From the curve fitting, the N1s band can be deconvoluted into two bands at around 399.5 eV (PN1) and 401.6 eV (PN2). The PN1 and PN2 correspond to pyridine-like and graphitic-like N.^{11,17} The pyridine-like N is referred to the N atoms that contribute to the system with a pair of pi electrons, whereas graphitic-like N

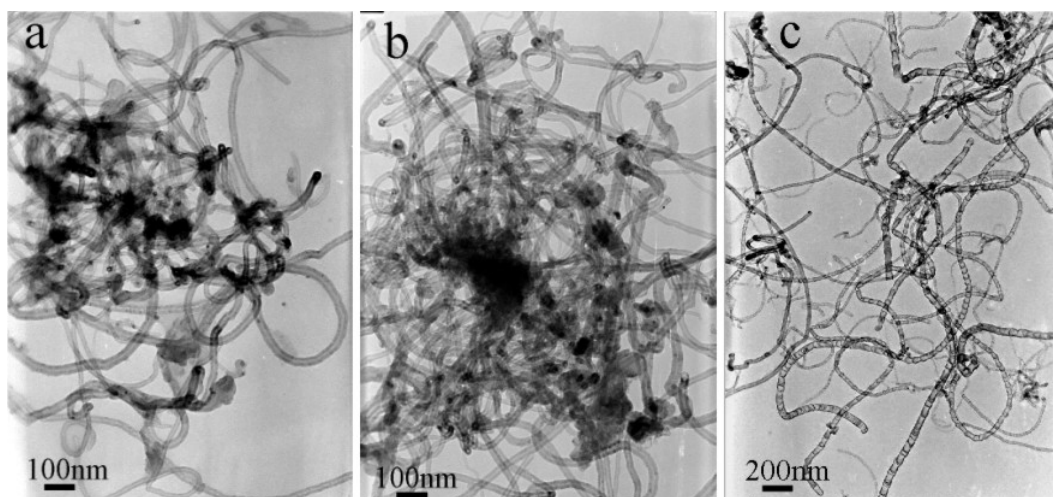


Figure 3. TEM micrographs for products with various catalysts: (a) $\text{Ni}_{1.07}\text{Mg}_{1.01}\text{AlO}_{3.58}$, (b) $\text{Ni}_{1.99}\text{Mg}_{0.29}\text{AlO}_{3.78}$ (c) $\text{Ni}_{2.31}\text{Mg}_{0.08}\text{AlO}_{3.89}$.

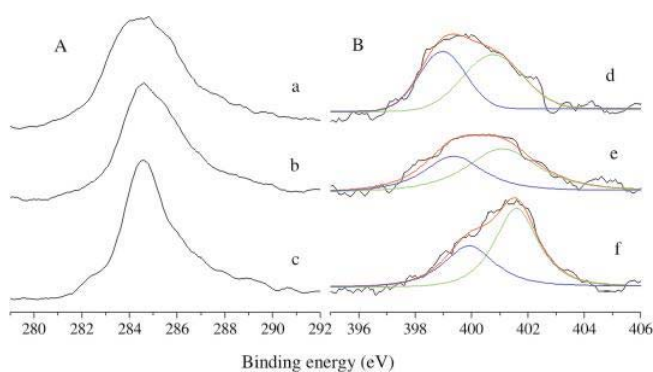


Figure 4. C1s (A) and N1s (B) XPS spectra of the CN_x nanotubes grown with various catalysts: (a), (d) $\text{Ni}_{1.07}\text{Mg}_{1.01}\text{AlO}_{3.58}$; (b), (e) $\text{Ni}_{1.99}\text{Mg}_{0.29}\text{AlO}_{3.78}$; (c), (f) $\text{Ni}_{2.31}\text{Mg}_{0.08}\text{AlO}_{3.89}$.

Table 1. The N content and the intensity of PN1 and PN2 structures for all the grown CN_x nanotubes with various catalysts.

Catalyst	N content (at.%)	The intensity of different N Structures (%)	
		PN1	PN2
$\text{Ni}_{1.07}\text{Mg}_{1.01}\text{AlO}_{3.58}$	5.4	46	54
$\text{Ni}_{1.99}\text{Mg}_{0.29}\text{AlO}_{3.78}$	6.6	42	58
$\text{Ni}_{2.31}\text{Mg}_{0.08}\text{AlO}_{3.89}$	8.8	38	62

corresponds to the coordinated N atoms substituting for C atoms in the graphene layers.¹³ There are several ways in which N can be incorporated in the CNT lattice¹⁸. However, there are only two ways observed in our studies as others have reported.^{11,17,19} The N content and intensity of PN1 and PN2 struc-

tures are listed in table 1. For catalysts with various Ni^{2+} content, the higher Ni^{2+} content, the higher N content and proportion of graphitic-like N structures can be obtained in the grown tubes.

We note that the tube morphology depends strongly on the N content. The tubes grown with $\text{Ni}_{2.31}\text{Mg}_{0.08}\text{AlO}_{3.89}$ have the N content of 8.8 at.% and all have an obvious bamboo-like morphology. However, an unobvious bamboo-like morphology exists in the tubes grown with $\text{Ni}_{1.07}\text{Mg}_{1.01}\text{AlO}_{3.58}$ and $\text{Ni}_{1.99}\text{Mg}_{0.29}\text{AlO}_{3.78}$, which have the N content of 5.4 and 6.6 at.%. So we can conclude that the higher N content, the more compartmentalized of tubes become, which is consistent with the early report.¹⁰ The higher N content also leads to the compartment layers in the tubes grown with $\text{Ni}_{2.31}\text{Mg}_{0.08}\text{AlO}_{3.89}$ becoming thicker and the distance between two adjacent compartment layers becoming longer. During the tube growing process, the compartment layers were bent and connected with the wall under less strain for the higher N content. After the joint, the sheets of compartment layers would grow eventually depart from the catalytic particles. If the stress were release, this joint growth would take longer before departing from the catalytic particle, resulting in less frequent formation of the thicker compartment layers.²⁰

The Raman spectra of the CN_x nanotubes with various catalysts are shown in figure 5. All spectra show mainly two bands at $\sim 1351\text{ cm}^{-1}$ (D-band) and $\sim 1580\text{ cm}^{-1}$ (G-band). The G band originates from the Raman active E_{2g} mode due to in-plane atomic displacements. The origin of D band has been explained as disorder-induced features due to the finite particle size effect or lattice distortion.²⁰ As the con-

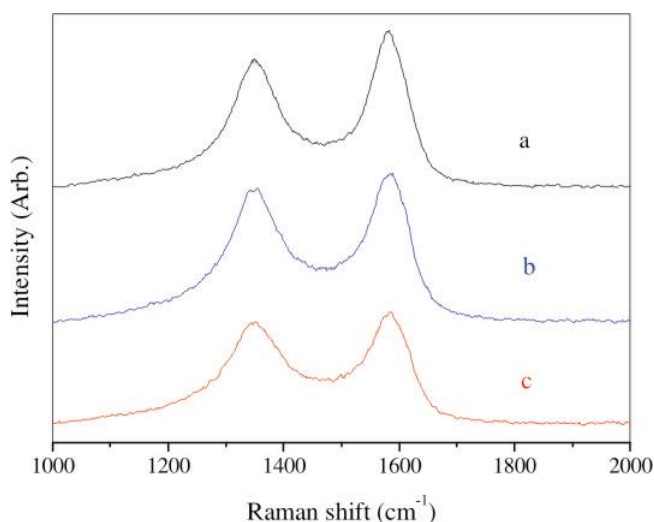


Figure 5. Raman spectrum for products with various catalysts: (a) $\text{Ni}_{1.07}\text{Mg}_{1.01}\text{AlO}_{3.58}$, (b) $\text{Ni}_{1.99}\text{Mg}_{0.29}\text{AlO}_{3.78}$ (c) $\text{Ni}_{2.31}\text{Mg}_{0.08}\text{AlO}_{3.89}$.

tent of Ni^{2+} in catalyst increases from $\text{Ni}_{1.07}\text{Mg}_{1.01}\text{AlO}_{3.58}$ to $\text{Ni}_{2.31}\text{Mg}_{0.08}\text{AlO}_{3.89}$, the $I_{\text{D}}/I_{\text{G}}$ value increase from 1.26 to 1.63. For the CN_x tubes grown with $\text{Ni}_{1.99}\text{Mg}_{0.29}\text{AlO}_{3.78}$, the $I_{\text{D}}/I_{\text{G}}$ value is 1.47. This suggests that more defects and disorders are introduced as the content of Ni^{2+} in catalyst increases. Based on the experimental results, it is believed that the defects and disorders are related to the presence of N in the CN_x tubes.

4. Conclusions

$\text{Ni}_{1.07}\text{Mg}_{1.01}\text{Al-LDH}$, $\text{Ni}_{1.99}\text{Mg}_{0.29}\text{Al-LDH}$, and $\text{Ni}_{2.31}\text{Mg}_{0.08}\text{Al-LDH}$ were prepared by introducing Ni^{2+} into the LDH layers. The CN_x nanotubes were synthesized using $\text{Ni}_{1.07}\text{Mg}_{1.01}\text{AlO}_{3.58}$, $\text{Ni}_{1.99}\text{Mg}_{0.29}\text{AlO}_{3.78}$, and $\text{Ni}_{2.31}\text{Mg}_{0.08}\text{AlO}_{3.89}$ mixed oxides as catalysts obtained by calcination of these LDH precursors. By control the content of Ni^{2+} in LDHs, the N content of 5.4 to 8.8 at.% in CN_x nanotubes was obtained. The higher Ni^{2+} content, the higher N content and proportion of graphitic-like N structures could be achieved. The tubes grown with $\text{Ni}_{2.31}\text{Mg}_{0.08}\text{AlO}_{3.89}$ had larger diameter and an obvious bamboo-like morphology, while an unobvious bamboo-like morphology existed in the tubes grown with $\text{Ni}_{1.07}\text{Mg}_{1.01}\text{AlO}_{3.58}$ and $\text{Ni}_{1.99}\text{Mg}_{0.29}\text{AlO}_{3.78}$. In addition, the compartment layers of the tubes grown with $\text{Ni}_{2.31}\text{Mg}_{0.08}\text{AlO}_{3.89}$ were thicker and had a longer distance than those grown with $\text{Ni}_{1.07}\text{Mg}_{1.01}\text{AlO}_{3.58}$ and $\text{Ni}_{1.99}\text{Mg}_{0.29}\text{AlO}_{3.78}$. The present result shows

that the control of morphology, N content and pyridine-like N structures for CN_x nanotubes can be achieved to a certain extent by varying the content of Ni^{2+} in LDH precursors.

Acknowledgements

This work is conducted with the financial support from the Chinese National '863' (No. 2006AA03Z570) fund and Excellent Young Scholars Research Fund of Beijing Institute of Technology (No. c2007YS0404).

References

1. Cavani F, Trifiro F and Vaccari A 1991 *Catal. Today* **11** 173
2. Zhao Y, Jiao Q Z, Li C H and Liang J 2007 *Carbon* **45** 2159
3. Odom T W, Huang J L, Kim P and Lieber C M 1998 *Nature* **391** 62
4. Fan S, Chapline M G, Franklin N R, Tomblor T W, Cassell A M and Dai H 1999 *Science* **283** 512
5. Bachtold A, Hadley P, Nakanishi T and Dekker C 2001 *Science* **294** 1317
6. Liang W, Bockrath M, Bozovic D, Hafner J H, Tinkham M and Park H 2001 *Nature* **411** 665
7. Hamada S, Sawasa S and Oshiyama A 1992 *Phys. Rev. Lett.* **68** 1579
8. Terrones M, Ajayan P M, Banhart F, Blase X, Carrol D L, Charlier J C, Crzerw R, Foley B, Grobert N, Kamalakaran R, Kohler-Redlich P, Ruhle M, Seeger T and Terrones H 2002 *Appl. Phys.* **A74** 355
9. Maldonado S, Morin S and Stevenson K J 2006 *Carbon* **44** 1429
10. Wang X B, Liu Y Q, Zhu D B, Zhang L, Ma H Z, Yao N and Zhang B L 2002 *J. Phys. Chem.* **B106** 2186
11. Wang E G, Guo Z G, Ma J, Zhou M M, Pu Y K, Liu S, Zhang G Y and Zhong D Y 2003 *Carbon* **41** 827
12. Jang J W and Lee C E 2004 *Appl. Phys. Lett.* **84** 2877
13. Tao X Y, Zhang X B, Sun F Y, Cheng J P, Liu F and Luo Z Q 2007 *Diamond Relat. Mater.* **16** 425
14. Kim N S, Lee Y T, Park J, Han J B, Choi Y S, Choi S Y, Choo J and Lee G H 2003 *J. Phys. Chem.* **B107** 9249
15. Choi H C and Park J 2005 *J. Phys. Chem.* **B109** 4333
16. Zhao Y, Liang J and Zhou X W 2005 *J. Adv. Mater.* **37** 11
17. Liu J W, Webster S and Carroll D L 2005 *J. Phys. Chem.* **B109** 15769
18. Shimoyama I, Wu G H, Sekiguchi T and Baba Y 2000 *Phys. Rev.* **B62** R6053
19. Yang Z X, Xia Y D and Mokaya R 2005 *Chem. Mater.* **17** 4502
20. Lee Y T, Kim N S, Bae S Y and Park J 2003 *J. Phys. Chem.* **B107** 12958